scientific reports

Check for updates

OPEN

Synchronization and dynamics of modified fractional order Kawasaki disease model with chaos stability control

Kottakkaran Sooppy Nisar[1,2], Muhammad Farman[3,4,5]✉, Khadija Jamil[6], Evren Hincal[3] & Aceng Sambas[4,7,8]

In this paper, fractional calculus has proven to be invaluable in disease transmission dynamics and the creation of control systems, among other real-world problems. To investigate vaccine and treatment dynamics for disease control, this work focuses on Kawasaki illness and uses a unique fractional operator called the modified Atangana-Baleanu-Caputo derivative. The stability analysis, positivity, boundedness, existence, and uniqueness, are treated for the proposed model with novel fractional operators. Additionally, it investigates the effects of different parameters on the reproductive number. It verifies the existence and uniqueness of the solutions to the suggested model using Banach fixed point and the Leray-Schauder nonlinear alternative theorem. Employs Lyapunov functions to determine the model equilibria analysis global stability. The numerical simulation and results utilized the two-step Lagrange interpolation approach at various fractional order values. The results are contrasted with those obtained using the widely recognized ABC method and comparisons are also made to show the effects of the proposed method for the epidemic system. This model advances beyond existing Kawasaki disease models by incorporating fractional-order dynamics, which capture memory effects and long-range dependencies in biological systems, offering more accurate representations of disease progression. The inclusion of chaos stability control provides novel insights into managing complex, nonlinear behaviors, enhancing both theoretical understanding and potential clinical applications.

Keywords Kawasaki disease model, Lyapunov function, Leray-Schauder nonlinear, Chaos control, MABC operator

Infants and young children are susceptible to Kawasaki disease (KD), an inflammatory illness that affects blood vessels throughout their bodies[1,2]. In pediatric populations across North America, Europe, and Japan, Kawasaki disease is presently regarded as the predominant etiology of acquired heart disease[3,4]. The prevailing consensus has shifted regarding childhood Kawasaki disease, as it is increasingly acknowledged that the cardiovascular sequelae associated with this condition may extend into adulthood[5,6]. Although the exact etiology of Kawasaki illness is still unknown, findings from our laboratory[7,8] and other laboratories[9,10] support the theory that it is most likely caused by a traditional antigen. In[11,12], it is reported that pediatric patients administered high-dose intravenous immunoglobulin exhibit a reduced likelihood of developing coronary arteritis and, more specifically, coronary artery aneurysms; in the absence of treatment, as many as 30% of these patients may develop such conditions. In 60–75% of Kawasaki disease patients, intravenous immunoglobulin (IVIG) treatment results in coronary artery aneurysms (CAA) regression[13,14]. Nevertheless, it is unclear how precisely IVIG lowers the

[1]Department of Mathematics, College of Science and Humanities in Al Kharj, Prince Sattam bin Abdulaziz University, 11942 Al Kharj, Saudi Arabia. [2]Hourani Center for Applied Scientific Research, Al-Ahliyya Amman University, Amman, Jordan. [3]Department of Mathematics, Faculty of Arts and Sciences, Near East University, 99138 Nicosia, Cyprus. [4]Faculty of Informatics and Computing, Universiti Sultan Zainal Abidin, Campus Besut, 22200 Terengganu, Malaysia. [5]Research Center of Applied Mathematics, Khazar University, Baku, Azerbaijan. [6]Institute of Mathematics, Khwaja Fareed University of Engineering and Information Technology, Rahim Yar Khan, Pakistan. [7]Department of Mechanical Engineering, Universitas Muhammadiyah Tasikmalaya, Tamansari Gobras, 46196 Tasikmalaya, Indonesia. [8]Artificial Intelligence for Sustainability and Islamic Research Center (AIRIS), Universiti Sultan Zainal Abidin, 21300 Gongbadak, Terengganu, Malaysia. ✉email: farmanlink@gmail.com

incidence of cardiovascular problems[15]. Around 15–20% of patients diagnosed with (KD) display suboptimal reactions to (IVIG) treatment, and individuals within this specific category exhibit a heightened likelihood of experiencing coronary artery aneurysms[16,17]. A diverse array of both congenital and acquired immune cell phenotypes has been correlated with the penetration of the vascular endothelial layer in Kawasaki disease. The presence of an aggregation of monocytes, macrophages, and neutrophils within the arterial vessel walls[18,19], in conjunction with activated $CD8^+$ T lymphocytes and IgA^+ plasma cells, is observed in the post-mortem human tissues subjected to immunohistochemical examination[20]. Pro-inflammatory cytokines, such as tumor necrosis factor (TNF) and interleukin-1 beta, are released by immune cells that permeate the host organism. These cytokines promote the growth of CAAs and damage to vascular endothelial cells[23,24]. In the most badly affected instances, Kawasaki disease is thought to be a medium-sized vasculitis that results in coronary artery aneurysms. Aortic, axillary, brachial, and iliac artery aneurysms can sporadically develop, and there may be systemic vascular involvement. It has not yet been documented if KD has an impact on microcirculation.

The utilization of fractional calculus in addressing practical issues, encompassing healthcare and a multitude of other domains, has attracted considerable interest from scholars worldwide. Atangana and Baleanu developed derivatives that incorporate non-local and non-singular kernels using the generalized Mittag-Leffler function[27]. The Atangana and Baleanu fractional operator was recently developed inside Caputo's theoretical framework[28]. A fractional-order model for managing toxin activity and fires caused by humans is presented in the article[29]. It integrates simulations and chaos control approaches. It uses a modified ABC operator to optimize the model performance in handling complex environmental dynamics. To better understand the spread and control of the virus,[30] investigates the stability and complicated dynamics of a COVID-19 epidemic model utilizing a non-singular Mittag-Leffler law kernel. The fractional-order epidemic models in life sciences, discussing their historical development, current applications, and future potential for more accurately modeling the spread and control of infectious diseases[31]. The dynamics and stability of a COVID-19 pandemic model under a harmonic mean type incidence rate are examined in[32] by fractional calculus analysis. The HBV epidemic model[33] uses a convex incidence rate and sensitivity analysis to determine the main factors affecting the virus's propagation. A fractional COVID-19 pandemic model[34] using real data from Pakistan and incorporates the ABC operator for improved modeling accuracy. It investigates the dynamics and potential interventions for controlling the spread. The Caputo-Fabrizio definition is used in study[35] to examine a fractional-order boost converter with inductive loads. It explores the system's behavior, stability, and performance under fractional-order dynamics. A fractional-order Zener model[36] for viscoelastic dampers, incorporating temperature-order equivalence to better capture the damping behavior. It focuses on improving the accuracy of modeling viscoelastic materials in engineering applications. Study[37] presents a fractional-order mathematical model for the COVID-19 outbreak, accounting for both symptomatic and asymptomatic transmissions. It analyzes the dynamics of the disease spread with fractional derivatives for more accurate predictions and control strategies. A fractal-fractional mathematical model to regulate the prevalence of tuberculosis[38], emphasizing stability conditions, simulations, and sensitivity analysis to evaluate the model performance in practical settings. The article[39] explores new bifurcation results for fractional-order octonion-valued neural networks that incorporate delays, examining how these delays affect the network dynamics and stability. In[40] author investigates bifurcation phenomena in fractional neural networks with multiple delays and proposes a control scheme to manage the complex dynamics and enhance network stability. The study[41] demonstrates the existence of chaotic behavior and stability regions in a piecewise modified ABC fractional-order leukemia model, validated through symmetric numerical simulations. The existence and uniqueness of solutions in a modified-ABC fractional-order smoking model[42], highlighting its applicability to real-world scenarios. The use of artificial intelligence in data analysis with error recognition to improve liver transplantation outcomes in HIV-AIDS patients[43], utilizing modified ABC fractional-order operators for enhanced precision. The research[44] proves the existence of solutions and introduces a numerical scheme for a generalized hybrid class of n-coupled modified ABC-fractional differential equations, demonstrating its effectiveness through a practical application.

The modified Atangana-Baleanu-Caputo derivative is significant for the Kawasaki disease model because it introduces a non-local, memory-dependent mechanism that better captures the disease persistence and relapse characteristics. This fractional approach allows the model to reflect the influence of past infection and immunity states on current disease dynamics, providing a more accurate depiction of Kawasaki disease progression and treatment response. The integration of fractional order derivatives into disease modeling represents a significant advancement in epidemiological research. By capturing complex dynamics through memory effects and non-local interactions, these models offer improved insights into disease behavior and control strategies. As demonstrated across various studies, including those on COVID-19[45] and hepatitis B[46], fractional calculus not only enhances model accuracy but also informs public health interventions effectively.

This study introduces a fractional-order Kawasaki disease model using the modified Atangana-Baleanu-Caputo derivative, which better captures the disease's persistent and recurrent nature compared to classical models. Analysis reveals that lower fractional orders correlate with more aggressive disease progression, while higher orders show a dampening effect on inflammation. The MABC model demonstrates superior accuracy in simulating Kawasaki disease dynamics compared to the standard ABC model. The findings suggest that manipulating fractional orders could offer potential control points for disease interventions. The previous study[23] utilized a classical integer-order model to investigate key interactions in the pathogenesis of Kawasaki disease. In contrast, this study presents a new fractional-order model of Kawasaki disease, employing the modified Atangana-Baleanu-Caputo (MABC) derivative. This approach effectively captures memory effects and complex immune interactions, thereby improving the accuracy of simulations related to the inflammatory processes. Additionally, the study explores chaos control and stability by using Lyapunov functions and fixed-point theorems to analyze equilibria and the uniqueness of solutions.

Section 1 of this article serves as an introduction, and Sect. 2 provides a general definition of the strategies that are offered. The suggested models that are positively invariant, with equilibrium points, reproductive potential, and sensitivity examined, are shown in Sect. 3. Part 4 evaluates the proposed model stability while accounting for Lyapunov stability. The discrete Kawasaki disease model chaos is examined in Sect. 5. In Sect. 6, fixed point theory is used to verify the existence and uniqueness of a system of solutions. In Sect. 7, the Atangana Baleanu in Caputo sense fractional order system is solved using a unique numerical method. Graphs representing the numerical results of the proposed model are presented in Sect. 8. The conclusion is given in the last section, number 9.

Basic concepts

In this section, we will look over some basic ideas.

Definition 2.1 [28]Let $w \in M([0,\mathscr{Q}])$ and $\eta \in (0,1)$,$\mathscr{Q} > 0$. The ABC fractional derivative of a function $w(t)$ defines it as

$$ {}_{0}^{ABC}D_{t}^{\eta}w(t) = \frac{AB(\eta)}{1-\eta}\int_{0}^{t}\frac{d}{d\upsilon}w(\upsilon)\wp_{\eta}\left(-\frac{\eta(t-\upsilon)}{1-\eta}\right)d\upsilon, \tag{1} $$

Definition 2.2 [28]The ABC fractional integral connected to the function $w(t)$ is conceptualized as follows:

$$ {}_{0}^{ABC}I_{t}^{\eta}w(t) = \frac{1-\eta}{AB(\eta)}g(t) + \frac{\eta}{AB(\eta)\Gamma(\eta)}\int_{0}^{t}w(\upsilon)(t-\upsilon)^{\eta-1}d\upsilon, \tag{2} $$

where $\eta \in (0,1)$ and

$$ AB(\eta) = 1-\eta+\frac{\eta}{\Gamma(\eta)}. \tag{3} $$

Definition 2.3 [28]The MABC derivative for $w \in L(0,\mathscr{Q})$ and $\eta \in (0,1)$ can be formulated as follows: Consider a function $x \in L(0,\mathscr{Q})$. For $0 < \eta < 1$, the MABC derivative is defined as

$$ {}^{MABC}D_{0}^{\eta}w(t) = \frac{AB(\eta)}{1-\eta}\left[w(t) - \wp_{\eta}(-q_{\eta}t^{\eta})w(0) - q_{\eta}\int_{0}^{t}(t-\upsilon)^{\eta-1}\wp_{\eta,\eta}\left(-q_{\eta}(t-\upsilon)^{\eta}\right)w(\upsilon)d\upsilon\right], \tag{4} $$

where $q_{\eta} = \frac{\eta}{1-\eta}$ and $AB(\eta) = 1-\eta+\frac{\eta}{\Gamma(\eta)}$.

The Laplace transform

$$ \mathscr{L}\left\{{}^{MABC}D_{t}^{\eta}w(t);u\right\} = \frac{AB(\eta)}{(1-\eta)}\frac{u^{\eta}\mathscr{L}\{x(t);u\} - u^{\eta-1}w(0)}{u^{\eta}+q_{\eta}}, \qquad \left|\frac{q_{\eta}}{u^{\eta}}\right| < 1. \tag{5} $$

Definition 2.4 [28]$w \in L(0,\mathscr{Q})$ and $\eta \in (0,1)$ MABC integral is

$$ {}^{MABC}I_{0}^{\eta}w(t) = \frac{AB(1-\eta)}{AB(\eta)}\left[w(t)-w(0)\right] + q_{\eta}\left[{}^{RL}I_{0}^{\eta}\left(w(t)-w(0)\right)\right]. \tag{6} $$

Definition 2.5 [28]For $w'(t) \in (0,\infty)$ and $\eta \in (0,1)$ we have

$$ {}^{MABC}I_{0}^{\eta}\ {}^{MABC}D_{0}^{\eta}w(t) = w(t)-w(0), \tag{7} $$

where $\eta \in (0,1)$ and $\mathscr{W}(\eta)$ satisfies a normalizing function $\mathscr{W}(1) = \mathscr{W}(0) = 1$.

Lemma 1: Let $\Omega \in \mathbb{R}^{+}$ be a differentiable function. Then,

$$ {}_{0}^{MABC}D_{t}^{\eta}\left[\mathscr{Q}(t) - \mathscr{Q}^{*} - \mathscr{Q}^{*}\ln\frac{\mathscr{Q}(t)}{\mathscr{Q}^{*}}\right] \leq \left(1-\frac{\mathscr{Q}^{*}}{\mathscr{Q}(t)}\right)\ {}_{0}^{MABC}D_{t}^{\eta}\left(\mathscr{Q}(t)\right),\ \mathscr{Q}^{*} \in \mathbb{R}^{+}. $$

Mathematical model

The Kawasaki disease model has been notably shaped by previous research[23]. A four-category classification system is explained by means of the modeling equations regarding the ways in which different concentrations impact endothelial cell function and the inflammatory response. These equations include elements including cellular proliferation, activation by vascular endothelial growth factors, depletion owing to inflammatory stimuli, and intrinsic apoptosis to adequately depict the dynamics of normal endothelial cell concentration (E). Furthermore, they yield insights into the dynamics of vascular endothelial growth factor (V), chemokines, and activated adhesion factors (C). Ultimately, the model evaluates the dynamics of inflammatory factor concentrations (P),

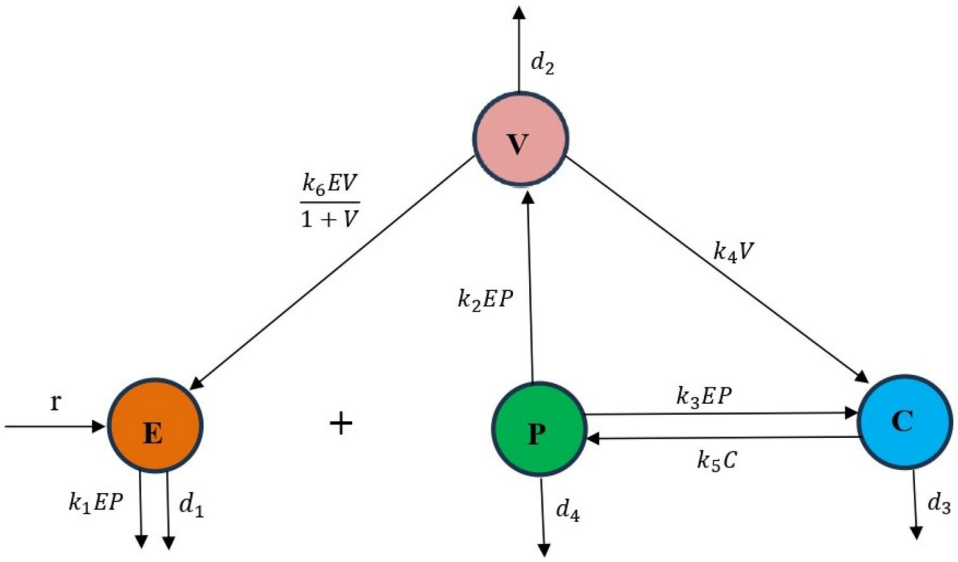

Fig. 1. Schematic diagram of the Kawasaki disease model.

Parameter	Biological meaning [23]	Value
r	Rate of normal endothelial cell proliferation	2
d_1	Normal endothelial cell apoptosis rates	0.5
d_2	Rate of endothelial growth factor hydrolysis	1
d_3	Adhesion factors and chemokines hydrolytic rate	1
d_4	Rate at which inflammatory factors hydrolyze	1
k_1	Injury rate of endothelial cells due to inflammatory factors	1
k_2	Production rate of endothelial growth factors due to inflammatory factors	0.1
k_3	Activated adhesion and chemokine production by inflammation	1
k_4	Adhesion and chemokine production by growth factors	0.5
k_5	Inflammatory factor production by activated immune cells	0.16
k_6	Endothelial cell growth promoted by factors	0.45

Table 1. Biological parameters and their meanings.

which are regulated by adhesion factors and the activation of immune cells represents in Figure 1. Biological parameters and their meanings are display in Table 1.

The fractional-order model is chosen for its ability to incorporate memory effects and long-range dependencies inherent in biological systems, which integer-order models cannot capture.

$$\begin{cases} {}_0^{MABC}D_t^{\eta}E(t) = r + \frac{k_6VE}{1+V} - k_1EP - d_1E, \\ {}_0^{MABC}D_t^{\eta}V(t) = k_2EP - d_2V, \\ {}_0^{MABC}D_t^{\eta}C(t) = k_3EP + k_4V - d_3C, \\ {}_0^{MABC}D_t^{\eta}P(t) = k_5C - d_4P, \end{cases} \tag{8}$$

under the initial conditions

$$E(0) \geq 0\,, \quad V(0) \geq 0\,, \quad C(0) \geq 0\,, \quad P(0) \geq 0. \tag{9}$$

Positively invariant

Lemma 2: The region $\gamma_l \in \mathbb{R}_+^4$

$$\gamma_l = \left\{(E, V, C, P) \in \mathbb{R}_+^4 : 0 \leq N\right\},$$

the system delineated in (8) in every solution, and the specified system within $\mathbb{R}_+^4$ exhibits positive invariance under the stipulation of non-negative.

Proof The following are the results from the (8) that we shall present:

$$\begin{aligned} {}_{0}^{MABC}D_t^{\eta}E(t)\,|_{E=0} &= r \geq 0,\\ {}_{0}^{MABC}D_t^{\eta}V(t)\,|_{V=0} &= k_2EP \geq 0,\\ {}_{0}^{MABC}D_t^{\eta}C(t)\,|_{C=0} &= k_3EP + k_4V \geq 0,\\ {}_{0}^{MABC}D_t^{\eta}P(t)\,|_{P=0} &= k_5C \geq 0. \end{aligned} \tag{10}$$

According to the system (10), the vector field is said to be localized in the region $\mathbb{R}_+^4$ on each hyperplane covering the non-negative orthant with $t \geq 0$. □

As $E(t) + V(t) + C(t) + P(t) = N$,. Each subpopulation is located in $[0, N]$, where the overall population N is assumed to be constant. Because of this, the subpopulation $E(t) + V(t) + C(t) + P(t)$ are also bounded.

Equilibrium points and R_0

The Kawasaki disease model disease-free points are $E^0 = (\frac{r}{d_1}, 0, 0, 0)$, and the Kawasaki disease model endemic equilibrium point is

$$E_* = \left(E^+, V^+, C^+, P^+\right),$$

$$E^+ = \frac{d_2d_3d_4}{d_2k_3k_5 + k_2k_4k_5},$$

$$V^+ = \frac{\sqrt{\mu} - d_2^2k_1k_3k_5 + k_2^2k_4k_5r - d_1d_2d_3d_4k_2 + d_2d_3d_4k_2k_6 - d_2k_1k_2k_4k_5 + d_2k_2k_3k_5r}{2d_2k_1k_5(d_2k_3 + k_2k_4)},$$

$$C^+ = \frac{\sqrt{\mu} - d_2^2k_1k_3k_5 + k_2^2k_4k_5r - d_1d_2d_3d_4k_2 + d_2d_3d_4k_2k_6 - d_2k_1k_2k_4k_5 + d_2k_2k_3k_5r}{2d_2d_3k_1k_2k_5},$$

$$P^+ = \frac{\sqrt{\mu} - d_2^2k_1k_3k_5 + k_2^2k_4k_5r - d_1d_2d_3d_4k_2 + d_2d_3d_4k_2k_6 - d_2k_1k_2k_4k_5 + d_2k_2k_3k_5r}{2d_2d_3d_4k_1k_2},$$

where

$$\begin{aligned} \mu = {} & d_1^2d_2^2d_3^2d_4^2k_2^2 - 2d_1d_2^3d_3d_4k_1k_2k_3k_5 - 2d_1d_2^2d_3^2d_4^2k_2^2k_6 - 2d_1d_2^2d_3d_4k_1k_2^2k_4k_5\\ & - 2d_1d_2^2d_3d_4k_2^2k_3k_5r - 2d_1d_2d_3d_4k_2^3k_4k_5r + d_2^4k_1^2k_3^2k_5^2 - 2d_2^3d_3d_4k_1k_2k_3k_5k_6\\ & + 2d_2^3k_1^2k_2k_3k_4k_5^2 + 2d_2^3k_1k_2k_3^2k_5^2r + d_2^2d_3^2d_4^2k_2^2k_6^2 - 2d_2^2d_3d_4k_1k_2^2k_4k_5k_6\\ & + 2d_2^2d_3d_4k_2^2k_3k_5k_6r + d_2^2k_1^2k_2^2k_4^2k_5^2 + 4d_2^2k_1k_2^2k_3k_4k_5^2r + d_2^2k_2^2k_3^2k_5^2r^2\\ & + 2d_2d_3d_4k_2^3k_4k_5k_6r + 2d_2k_1k_2^3k_4^2k_5^2r\\ & + 2d_2k_2^3k_3k_4k_5^2r^2 + k_2^4k_4^2k_5^2r^2. \end{aligned}$$

In the modified fractional-order Kawasaki disease model, the reproduction number is crucial for assessing the potential spread of the disease within a population.

Let

$$F = \begin{bmatrix} 0 & 0 & k_2\frac{r}{d_1}\\ 0 & 0 & k_3\frac{r}{d_1}\\ 0 & 0 & 0 \end{bmatrix},$$

$$V = \begin{bmatrix} d_2 & 0 & 0\\ -k_4 & d_3 & 0\\ 0 & -k_5 & d_4 \end{bmatrix}.$$

In particular, FV^1 represents the spectral radius of the next generation matrix, which is the reproductive number.

$$FV^{-1} = \begin{bmatrix} \frac{k_2k_4k_5r}{d_1d_2d_3d_4} & \frac{k_2k_5r}{d_1d_3d_4} & \frac{k_2r}{d_1d_4} & 0\\ \frac{k_3k_4k_5r}{d_1d_2d_3d_4} & \frac{k_3k_5r}{d_1d_3d_4} & \frac{k_3r}{d_1d_4} & 0\\ 0 & 0 & 0 & 0\\ 0 & 0 & 0 & 0 \end{bmatrix},$$

$$R_0 = \frac{rk_5\left(k_2k_4 + k_3d_2\right)}{d_1d_2d_3d_4}. \tag{11}$$

It is widely recognized that when $R_0 < 1$, the transmission of the infection will ultimately cease. Conversely, the disease will propagate throughout the population if $R_0 > 1$. Figure 2 shows the impact of several parameters on R_0.

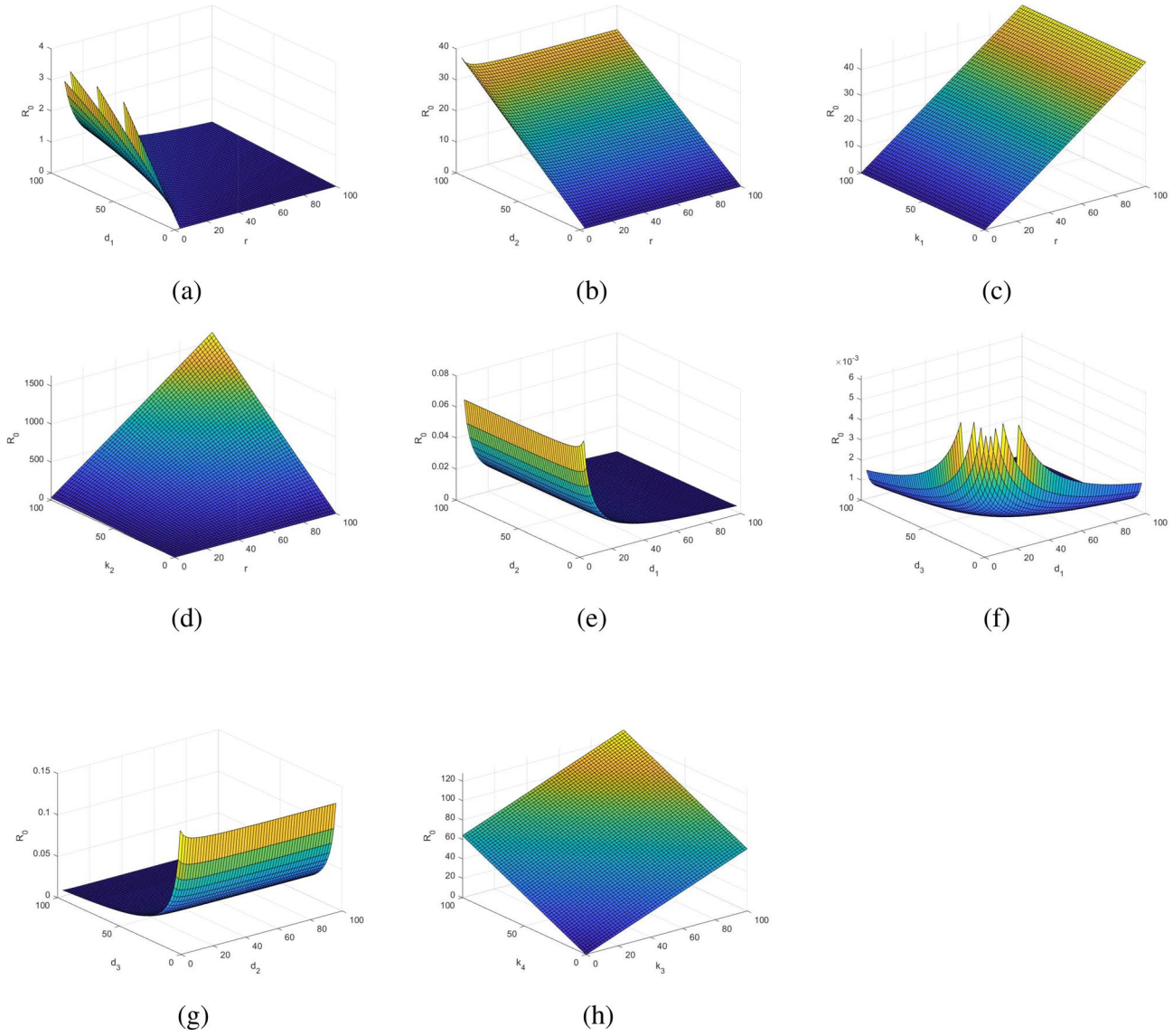

Fig. 2. Impact of several parameters on R_0.

Sensitivity snalysis

Sensitivity analysis demonstrates that fractional-order parameters significantly influence system stability, offering deeper insights into disease progression. These advantages highlight the fractional-order model's superior capability in modeling Kawasaki disease dynamics. The sensitivity of R_0 is following.

$$\frac{\partial R_0}{\partial r} = \frac{d_2k_3k_5 + k_2k_4k_5}{d_1d_2d_3d_4} > 0,$$

$$\frac{\partial R_0}{\partial d_1} = -\frac{d_2k_3k_5r + k_2k_4k_5r}{d_1^2d_2d_3d_4} < 0,$$

$$\frac{\partial R_0}{\partial d_2} = \frac{k_3k_5r}{d_1d_2d_3d_4} - \frac{d_2k_3k_5r + k_2k_4k_5r}{d_1d_2^2d_3d_4} < 0,$$

$$\frac{\partial R_0}{\partial d_3} = -\frac{d_2k_3k_5r + k_2k_4k_5r}{d_1d_2d_3^2d_4} < 0,$$

$$\frac{\partial R_0}{\partial d_4} = -\frac{d_2k_3k_5r + k_2k_4k_5r}{d_1d_2d_3d_4^2} < 0,$$

$$\frac{\partial R_0}{\partial k_2} = \frac{k_4k_5r}{d_1d_2d_3d_4} > 0,$$

$$\frac{\partial R_0}{\partial k_3} = \frac{k_5 r}{d_1 d_3 d_4} > 0,$$
$$\frac{\partial R_0}{\partial k_4} = \frac{k_2 k_5 r}{d_1 d_2 d_3 d_4} > 0,$$
$$\frac{\partial R_0}{\partial k_5} = \frac{d_2 k_3 r + k_2 k_4 r}{d_1 d_2 d_3 d_4} > 0.$$

Positive sensitivity indices are associated with an elevation of R_0, whereas negative indices are correlated with a reduction in this value. The sensitivity index is linked to the R_0 parameter. Figure 3 elucidates critical elements that affect transmission potential, thereby facilitating the discernment of essential variables and their implications on the propagation of Kawasaki disease. Parameters like r, k_2, k_3, k_4, and k_5 in Figure 3 have a positive sensitivity index and positively affect R_0. Increasing r, k_2, k_3, k_4, and k_5 can either increase the value of R_0 or cause an outbreak. However, parameters with a negative sensitivity index, such as d_1, d_2, d_3, and d_4, have a negative impact on reducing the disease's progress.

Stability analysis

To enhance comprehension of the dynamic features of the suggested model system (8) and the ways in which control strategies impact the dynamics of infectious disease transmission, a qualitative analysis of the system is conducted. The infectious model stability features are examined first.

Local stability

Theorem 4.1 An equilibrium free E^0 of the Kawasaki disease exhibits asymptotic local stability when $R_0 < 1$. Unstability exists if $R_0 > 1$.

Proof For the system (8) at E_0, the Jacobian can be expressed as

$$\begin{bmatrix} \frac{k_6 V}{1+V} - k_1 P - d_1 & \frac{E k_6}{1+V} - \frac{E V k_6}{(V+1)^2} & 0 & -k_1 E \\ k_2 P & -d_2 & 0 & k_2 E \\ k_3 P & k_4 & -d_3 & k_3 E \\ 0 & 0 & k_5 & -d_4 \end{bmatrix}.$$

Verifying that each and every eigenvalue of the matrix $J(E^0)$ satisfies the stability condition is both necessary and sufficient for the equilibrium point E^0 to be locally asymptotically stable:

$$|\arg(\lambda_i)| > \frac{\eta\pi}{2}. \tag{12}$$

Jacobian matrix has the following eigenvalues: $\lambda_1 = -0.5, \lambda_2 = -0.1305, \lambda_3 = -1.4347, \lambda_4 = -1.4347$. It is obvious that the point E^0 is locally asympotically stable if $R_0 < 1$and all the eigenvalues of $J(E^0)$ are negative. □

Global stability

Lyapunov first derivative

For the endemic Lyapunov function, $\{E, V, P, C\}$, ${}_0^{MABC}D_t^{\eta} L < 0$, is the endemic equilibrium E_*.

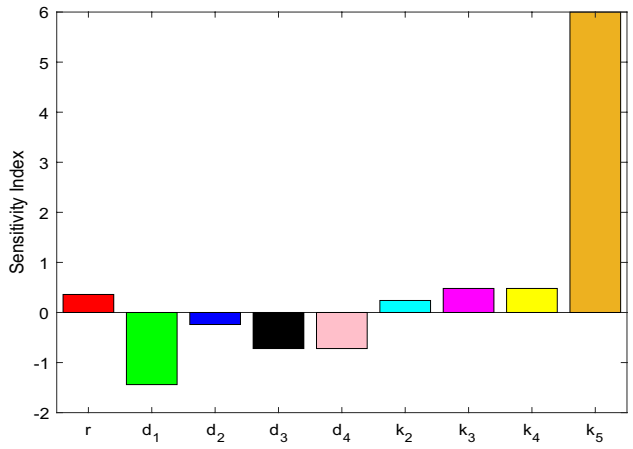

Fig. 3. sensitivity indices of variables in R_0.

Theorem 4.2 The endemic equilibrium points E_*, in the Kawasaki disease model are globally asymptotically stable when $R_0 > 1$.

Proof The Lyapunov function is expressed as follows:

$$L(E^*, V^*, C^*, P^*) = \left(E - E^* - E^* \log \frac{E}{E^*}\right) + \left(V - V^* - V^* \log \frac{V}{V^*}\right) + \left(C - C^* - C^* \log \frac{C}{C^*}\right) + \left(P - P^* - P^* \log \frac{P}{P^*}\right). \tag{13}$$

Using Lemma 1 and taking modified ABC derivative, we get

$${}_0^{MABC}D_t^{\eta} L \leq \left(\frac{E - E^*}{E}\right) {}_0^{MABC}D_t^{\eta} E + \left(\frac{V - V^*}{V}\right) {}_0^{MABC}D_t^{\eta} V + \left(\frac{C - C^*}{C}\right) {}_0^{MABC}D_t^{\eta} C + \left(\frac{P - P^*}{P}\right) {}_0^{MABC}D_t^{\eta} P. \tag{14}$$

Using system (8) we get,

$${}_0^{MABC}D_t^{\eta} L \leq \left(\frac{E - E^*}{E}\right)\left(r + \frac{k_6 V E}{1+V} - k_1 E P - d_1 E\right) + \left(\frac{V - V^*}{V}\right)(k_2 E P - d_2 V) + \left(\frac{C - C^*}{C}\right)(k_3 E P + k_4 V - d_3 C) + \left(\frac{P - P^*}{P}\right)(k_5 C - d_4 P). \tag{15}$$

Putting $E = E - E^*, V = V - V^*, C = C - C^*$ and $P = P - P^*$ leads to.

$$\begin{aligned}
{}_0^{MABC}D_t^{\eta} L \leq{}& \left(\frac{E - E^*}{E}\right)\left(r + \frac{k_6 (V - V^*)(E - E^*)}{1 + (V - V^*)} - k_1 (E - E^*)(P - P^*) - d_1 (E - E^*)\right) \\
&+ \left(\frac{V - V^*}{V}\right)(k_2 (E - E^*)(P - P^*) - d_2 (V - V^*)) \\
&+ \left(\frac{C - C^*}{C}\right)(k_3 (E - E^*)(P - P^*) + k_4 (V - V^*) - d_3 (C - C^*)) \\
&+ \left(\frac{P - P^*}{P}\right)(k_5 (C - C^*) - d_4 (P - P^*)),
\end{aligned}$$

$$\begin{aligned}
{}_0^{MABC}D_t^{\eta} L \leq{}& \left(\frac{E - E^*}{E}\right) r + \frac{k_6 (E - E^*)^2 V}{E(1 + (V - V^*))} - \frac{k_6 (E - E^*)^2 V^*}{E(1 + (V - V^*))} + \frac{(E - E^*)^2}{E} k_1 P^* \\
&- \frac{(E - E^*)^2}{E} k_1 P + \left(\frac{V - V^*}{V}\right) k_2 E P - \left(\frac{V - V^*}{V}\right) k_2 E P^* - \left(\frac{V - V^*}{V}\right) k_2 E^* P \\
&+ \left(\frac{V - V^*}{V}\right) k_2 E^* P^* + \left(\frac{C - C^*}{C}\right) k_3 E P - \left(\frac{C - C^*}{C}\right) k_3 E P^* - \left(\frac{C - C^*}{C}\right) k_3 E^* P \\
&+ \left(\frac{C - C^*}{C}\right) k_3 E^* P^* - \frac{(C - C^*)^2}{C} d_3 + \left(\frac{P - P^*}{P}\right) k_2 C - \left(\frac{P - P^*}{P}\right) k_2 C^* - \frac{(P - P^*)^2}{P} d_4.
\end{aligned}$$

Now, we write

$${}_0^{MABC}D_t^{\eta} L \leq \theta - \phi,$$

$$\begin{aligned}
\theta ={}& \left(\frac{E - E^*}{E}\right) r + \frac{k_6 (E - E^*)^2 V}{E(1 + (V - V^*))} + \frac{(E - E^*)^2}{E} k_1 P^* + \left(\frac{V - V^*}{V}\right) k_2 E P + \left(\frac{V - V^*}{V}\right) k_2 E^* P^* \\
&+ \left(\frac{C - C^*}{C}\right) k_3 E P + \left(\frac{C - C^*}{C}\right) k_3 E^* P^* + \left(\frac{P - P^*}{P}\right) k_2 C,
\end{aligned}$$

$$\begin{aligned}
\phi ={}& \frac{k_6 (E - E^*)^2 V^*}{E(1 + (V - V^*))} + \frac{(E - E^*)^2}{E} k_1 P + \frac{(E - E^*)^2}{E} d_1 + \left(\frac{V - V^*}{V}\right) k_2 E P^* + \left(\frac{V - V^*}{V}\right) k_2 E^* P \\
&+ \frac{(V - V^*)^2}{V} d_2 + \left(\frac{C - C^*}{C}\right) k_3 E P^* + \left(\frac{C - C^*}{C}\right) k_3 E^* P + \frac{(C - C^*)^2}{C} d_3 \\
&+ \left(\frac{P - P^*}{P}\right) k_2 C^* + \frac{(P - P^*)^2}{P} d_4.
\end{aligned}$$

It is achieved that if $\theta < \phi$, this yields ${}_0^{MABC}D_t^{\eta} L < 0$, however when $E = E^*, V = V^*, C = C^* and P = P^*$.

$$0 = \theta - \phi \quad \Rightarrow \quad {}_0^{MABC}D_t^{\eta} L = 0. \tag{16}$$

It is possible to demonstrate the proposed model largest compact invariant set.

$$\{(E^*, V^*, C^*, P_h^*)\}. \tag{17}$$

By employing the Lasalles invariance principle if the system is stable then E^* is also stable within it. □

Remark 1 Fractional-order derivatives in Lyapunov functions affect stability criteria by introducing a memory-dependent behavior, reflecting past states in the stability analysis, unlike standard integer-order systems. This added memory component allows for slower convergence rates, which captures the persistent and recurrent nature of Kawasaki disease dynamics more accurately.

Existence criteria

Lemma 5.1 The initial equation of the MABC-FDE framework, denoted as equation (8), encompasses solutions of a nature that is elucidated in the subsequent discussion.

$$\begin{aligned} E(t) = E(0) + \mathscr{Q}\beth_1(t, E(t)) + \mathscr{Z}\int_0^t (t-\upsilon)^{\eta-1}\beth_1(\upsilon, E(\upsilon))\, d\upsilon \\ - \mathscr{Q}\beth_1(0, E(0))\left(1 + \frac{\Psi_\eta}{\Gamma(\eta+1)}t^{\eta}\right), \end{aligned} \tag{18}$$

where

$$\mathscr{Q} = \frac{1-\eta}{\mathscr{B}(\eta)},$$

$$\mathscr{Z} = \frac{\eta}{\mathscr{B}(\eta)\Gamma(\eta)}.$$

Simlerly, for others, where

$$\begin{aligned} &\beth_1(t, E(t)) = r + \tfrac{k_6 VE}{1+V} - k_1 EP - d_1 E, \\ &\beth_2(t, V(t)) = k_2 EP - d_2 V, \\ &\beth_3(t, C(t)) = k_3 EP + k_4 V - d_3 C, \\ &\beth_4(t, P(t)) = k_5 C - d_4 P. \end{aligned}$$

A solution for the modified ABC model is determined based on the following assumptions:

$\mathscr{W}^\star$ Consider $E, \bar{E}, V, \bar{V}, C, \bar{C}, P, \bar{P} \in \mathbb{L}[0,1]$, is a continuous function with the higher limit, show that $\|E\| \leq \daleth_1$, $\|V\| \leq \daleth_2$, $\|C\| \leq \daleth_3$, $\|P\| \leq \daleth_4$, where $\daleth_1, \daleth_2, \daleth_3, \daleth_4$ are made up only of positive constants. To elucidate further, let us suppose that: $\gimel_1 = \left(\frac{k_6\daleth_2}{1+\daleth_2} - k_1\daleth_4 - d_1\right)$, $\daleth_2 = -d_2$, $\daleth_3 = -d_3$ and $\daleth_4 = -d_4$.

Theorem 5.2 The $\beth_j$ indexed by j within the domain N_1^4 will adhere to the Lipschitz condition contingent upon the veracity of the assumption $\mathscr{W}^\star$, provided that all $\gimel_j$ are less than 1 for each j in the specified set.

Proof We start by proving that the function $\beth_1(t, E)$ satisfies the Lipschitz condition. The implication of $\mathscr{W}^\star$, which we have, is used to achieve this.

$$\begin{aligned} \left\|\beth_1(t, E) - \beth_1\left(t, \bar{E}\right)\right\| &= \left\|\left(\frac{k_6 V}{1+V} - k_1 P - d_1\right)E - \left(\frac{k_6 V}{1+V} - k_1 P - d_1\right)\bar{E}\right\| \\ &\leq \frac{k_6\|V\|}{1+\|V\|}\left\|E - \bar{E}\right\| - k_1\|P\|\left\|E - \bar{E}\right\| - d_1\left\|E - \bar{E}\right\| \\ &\leq \left(\frac{k_6\daleth_2}{1+\daleth_2} + k_1\daleth_4 + d_1\right)\|E - E\| \\ &= \gimel_1\left\|E - \bar{E}\right\|, \end{aligned} \tag{19}$$

$\beth_1 = \left(\frac{k_6\daleth_2}{1+\daleth_2} + k_1\daleth_4 + d_1\right)$.

$$\begin{aligned}\left\|\beth_2(t,V)-\beth_2\left(t,\bar{V}\right)\right\| &= \left\|(-d_2)V-(-d_2)\bar{V}\right\| \\ &\leq d_2\left\|V-\bar{V}\right\| \\ &= \daleth_2\left\|V-\bar{V}\right\|,\end{aligned} \tag{20}$$

$\daleth_2 = d_2$.

$$\begin{aligned}\left\|\beth_3(t,C)-\beth_3\left(t,\bar{C}\right)\right\| &= \left\|(-d_3)C-(-d_3)\bar{C}\right\| \\ &\leq d_3\left\|C-\bar{C}\right\| \\ &= \daleth_3\left\|C-\bar{C}\right\|,\end{aligned} \tag{21}$$

$\daleth_3 = d_3$.

$$\begin{aligned}\left\|\beth_4(t,P)-\beth_4\left(t,\bar{P}\right)\right\| &= \left\|(-d_4)P-(-d_4)\bar{P}\right\| \\ &\leq d_4\left\|P-\bar{P}\right\| \\ &= \zeta_4\left\|P-\bar{P}\right\|,\end{aligned} \tag{22}$$

$\daleth_4 = d_4$. **It can be discerned that the Lipschitz condition is fulfilled by the elements $\beth_1, \beth_2, \beth_3, \beth_4$. Furthermore, it can be conclusively shown that each of the $\beth_j$ for $j = 1, 2, 3, 4$ adheres to the Lipschitz condition, thereby corroborating their legitimacy, as derived from equations (19) to (22).**

Suppose there is a

$$\begin{aligned}E(t) = E(0) &+ \mathscr{Q}\beth_1(t,E(t)) + \mathscr{Z}\int_0^t (t-\upsilon)^{\eta-1}\beth_1(\upsilon,E(\upsilon))\,d\upsilon \\ &- \mathscr{Q}\beth_{1_0}(t,E(t))\left(1+\frac{\Psi_\eta}{\Gamma(\eta+1)}t^\eta\right),\end{aligned} \tag{23}$$

The next stage is to define the recursive formulae for the model, which is listed as follows:

$$\begin{aligned}E_{n+1}(t) - E(0) &= \mathscr{Q}\beth_1(t,E_n(t)) + \mathscr{Z}\int_0^t (t-\upsilon)^{\eta-1}\beth_1(\upsilon,E_n(\upsilon))\,d\upsilon \\ &- \mathscr{Q}\beth_{1_0}(t,E(t))\left(1+\frac{\Psi_\eta}{\Gamma(\eta+1)}t^\eta\right).\end{aligned} \tag{24}$$

In a same pattern we solve for V,C,P. □

Theorem 5.3 Should the veracity of the forthcoming assertion be substantiated, then the MABC Kawasaki disease (8) presents a solution predicated on the premise that $\mathscr{W}^\star$ must be affirmed as accurate.

$$\Upsilon_1 = \max\left[\daleth_1, \daleth_2, \daleth_3, \daleth_4\right] < 1.$$

Proof We define function as follows:

$$\begin{aligned}&\mathscr{E}1_n(t) = E_{n+1}(t) - E(t),\\ &\mathscr{E}2_n(t) = V_{n+1}(t) - V(t),\\ &\mathscr{E}3_n(t) = C_{n+1}(t) - C(t),\\ &\mathscr{E}4_n(t) = P_{n+1}(t) - P(t),\end{aligned}$$

$$
\begin{aligned}
\|\mathscr{E}1_n\| &= \left\| \mathscr{Q}\mathfrak{Z}_1\left(t, E_n(t)\right) + \mathscr{Z}\int_0^t (t-\upsilon)^{\eta-1}\mathfrak{Z}_1\left(\upsilon, E_n(\upsilon)\right)d\upsilon - \mathscr{Q}\mathfrak{Z}_1^0\left(t, E(t)\right)\left(1+\frac{\Psi_\eta}{\Gamma(\eta+1)}t^\eta\right)\right. \\
&\quad \left. - \left[\mathscr{Q}\mathfrak{Z}_1\left(t, E(t)\right) + \mathscr{Z}\int_0^t (t-\upsilon)^{\eta-1}\mathfrak{Z}_1\left(\upsilon, E(\upsilon)\right)d\upsilon - \mathscr{Q}\mathfrak{Z}_1^0\left(t, E(t)\right)\left(1+\frac{\Psi_\eta}{\Gamma(\eta+1)}t^\eta\right)\right]\right\| \\
&= \mathscr{Z}\int_0^t (t-\upsilon)^{\eta-1}\left\|\mathfrak{Z}_1\left(\upsilon, E_n(\upsilon)\right) - \mathfrak{Z}_1\left(\upsilon, E(\upsilon)\right)\right\|d\upsilon + \mathscr{Q}\left\|\mathfrak{Z}_1\left(t, E_n(t)\right) - \mathfrak{Z}_1\left(t, E(t)\right)\right\| \\
&\le \mathscr{Z}\int_0^t (t-\upsilon)^{\eta-1}\urcorner_1\left\|E_{n-1} - E\right\|d\upsilon + \mathscr{Q}\urcorner_1\left\|E_{n-1} - E\right\| \\
&\le \left[\mathscr{S} + \mathscr{Q}\right]\urcorner_1\left\|E_{n-1} - E\right\| \\
&\le \left[\mathscr{S} + \mathscr{Q}\right]^n\urcorner_1^n\left\|E_{n-1} - E\right\|,
\end{aligned} \tag{25}
$$

$$
\mathscr{S} = \frac{\eta}{\mathscr{B}(\eta)\,\Gamma(\eta+1)},
$$

where $\urcorner < 1$ and $n \to \infty$, $E_n \to E$ similarly we have

$$
\|\mathscr{E}2_n\| \le \left[\mathscr{S} + \mathscr{Q}\right]^n\urcorner_2^n\left\|V_{n-1} - V\right\|, \tag{26}
$$

$$
\|\mathscr{E}3_n\| \le \left[\mathscr{S} + \mathscr{Q}\right]^n\urcorner_3^n\left\|C_{n-1} - C\right\|, \tag{27}
$$

$$
\|\mathscr{E}4_n\| \le \left[\mathscr{S} + \mathscr{Q}\right]^n\urcorner_4^n\left\|P_{n-1} - P\right\|, \tag{28}
$$

Due to the fact that $\mathscr{E}j_n(t) \to 0$ as $n \to \infty$ for $j \in N_1^4$ and $\urcorner < 1$, Hence prove is done.

Theorem 5.4 If the following statement is true, then the unique solution given by the MABC model (8) is:

$$
\left[\mathscr{S} + \mathscr{Q}\right]\urcorner_j \le 1, j \in N_1^4.
$$

Proof We may look at $\bar{E}(t)$, $\bar{V}(t)$, $\bar{C}(t)$, and $\bar{P}(t)$ as potential alternatives. Following that, we have:

$$
\begin{aligned}
\bar{E}(t) &= \bar{E}(0) + \mathscr{Q}\mathfrak{Z}_1\left(t, \bar{E}(t)\right) + \mathscr{Z}\int_0^t (t-\upsilon)^{\eta-1}\mathfrak{Z}_1\left(\upsilon, \bar{E}(\upsilon)\right)d\upsilon \\
&\quad - \mathscr{Q}\mathfrak{Z}_{1_0}\left(t, \bar{E}(t)\right)\left(1+\frac{\Psi_\eta}{\Gamma(\eta+1)}t^\eta\right),
\end{aligned} \tag{29}
$$

□

Likewise, for additional compartments

$$
\begin{aligned}
\left\|E-\bar{E}\right\| &= \left\| \mathscr{Q}\beth_1\left(t,E\left(t\right)\right)+\mathscr{Z}\int_0^t\left(t-\upsilon\right)^{\eta-1}\beth_1\left(\upsilon,E\left(\upsilon\right)\right)d\upsilon \right. \\
&\quad -\mathscr{Q}\beth_{1_0}\left(t,E\left(t\right)\right)\left(1+\frac{\Psi_\eta}{\Gamma\left(\eta+1\right)}t^\eta\right) \\
&\quad -\left[\mathscr{Q}\beth_1\left(t,\bar{E}\left(t\right)\right)+\mathscr{Z}\int_0^t\left(t-\upsilon\right)^{\eta-1}\beth_1\left(\upsilon,\bar{E}\left(\upsilon\right)\right)d\upsilon\right. \\
&\quad \left.\left.-\mathscr{Q}\beth_{1_0}\left(t,\bar{E}\left(t\right)\right)\left(1+\frac{\Psi_\eta}{\Gamma\left(\eta+1\right)}t^\eta\right)\right] \\
&= \mathscr{Z}\int_0^t\left(t-\upsilon\right)^{\eta-1}\left\|\beth_1\left(\upsilon,E\left(\upsilon\right)\right)-\beth_1\left(\upsilon,\bar{E}\left(\upsilon\right)\right)\right\|d\upsilon \\
&\quad +\mathscr{Q}\left\|\beth_1\left(t,E\left(t\right)\right)-\beth_1\left(t,\bar{E}\left(t\right)\right)\right\| \\
&\leq \mathscr{Z}\int_0^t\left(t-\upsilon\right)^{\eta-1}\urcorner_1\left\|E-\bar{E}\right\|d\upsilon+\mathscr{Q}\beth_1\left\|E-\bar{E}\right\| \\
&\leq \left[\mathscr{S}+\mathscr{Q}\right]\urcorner_1\left\|E-\bar{E}\right\|,
\end{aligned}
\tag{30}
$$

and so

$$
\left[1-\mathscr{S}+\mathscr{Q}\urcorner_1\right]\quad\left\|E\quad-\bar{E}\right\|\leq 0, \tag{31}
$$

when $\left\|E-\bar{E}\right\|=0$, the inequality (46) is true, E must equal $\bar{E}$. In a comparable direction, we have

$$
\left[1-\mathscr{S}+\mathscr{Q}\urcorner_2\right]\quad\left\|V\quad-\bar{V}\right\|\leq 0, \tag{32}
$$

$$
\left[1-\mathscr{S}+\mathscr{Q}\urcorner_3\right]\quad\left\|C\quad-\bar{C}\right\|\leq 0, \tag{33}
$$

$$
\left[1-\mathscr{S}+\mathscr{Q}\urcorner_4\right]\quad\left\|P\quad-\bar{P}\right\|\leq 0, \tag{34}
$$

Therefore, the solution produced by the Kawasaki disease exhibits the property of uniqueness.

Chaos control

In this section, we use the linear feedback control method to stabilize system (8) to its equilibrium positions. The fractional-order system in its controlled form (8) will be examined as follows:

$$
\begin{aligned}
{}_0^{MABC}D_t^\eta E(t) &= r+\tfrac{k_6VE}{1+V}-k_1EP-d_1E-w_1(E-E_1),\\
{}_0^{MABC}D_t^\eta V(t) &= k_2EP-d_2V-w_2\left(V-V_1\right),\\
{}_0^{MABC}D_t^\eta C(t) &= k_3EP+k_4V-d_3C-w_3\left(C-C_1\right),\\
{}_0^{MABC}D_t^\eta P(t) &= k_5C-d_4P-w_4\left(P-P_4\right),
\end{aligned}
\tag{35}
$$

where w_1, w_2, w_3, w_4 are control variables, and the system equilibrium point is E^0(8). For the system (35), the Jacobian matrix at E^0 is derived as

$$
J(E^0)=\begin{bmatrix}
-d_1-w1 & \frac{k_6r}{d_1} & 0 & -\frac{k_1r}{d_1}\\
0 & -d_2-w2 & 0 & \frac{k_2r}{d_1}\\
0 & k_4 & -d_3-w3 & \frac{k_3r}{d_1}\\
0 & 0 & k_5 & -d_4-w4
\end{bmatrix}.
$$

The characteristic equation of the Jacobian matrix $J(E^0)$ is given by

$$
f(\lambda)=\begin{vmatrix}
\lambda+d_1+w1 & -\frac{k_6r}{d_1} & 0 & \frac{k_1r}{d_1}\\
0 & \lambda+d_2+w2 & 0 & -\frac{k_2r}{d_1}\\
0 & -k_4 & \lambda+d_3+w3 & -\frac{k_3r}{d_1}\\
0 & 0 & -k_5 & \lambda+d_4+w4
\end{vmatrix}=0,
$$

characteristic polynomial of for the equilibrium point E^0 is given as

$$
C\left(\lambda\right)=\lambda^4+K_1^*\lambda^3+K_2^*\lambda^2+K_3^*\lambda+K_4^*, \tag{36}
$$

$$\begin{aligned} K_1^* &= \tfrac{c+d}{d_1} + \tfrac{(d_1+w_1)(a+b)}{d_1}, \\ K_2^* &= \tfrac{a+b}{d_1} + \tfrac{(d_1+w_1)(d_1d_2+d_1d_3+d_1d_4+d_1w_2+d_1w_3+d_1w_4)}{d_1}, \\ K_3^* &= d_1 + w_1 + \tfrac{d_1d_2+d_1d_3+d_1d_4+d_1w_2+d_1w_3+d_1w_4}{d_1}, \\ K_4^* &= \tfrac{(d_1+w_1)(c+d)}{d_1}, \end{aligned} \tag{37}$$

where

$$\begin{aligned} a &= d_1d_2d_3 + d_1d_2d_4 + d_1d_3d_4 + d_1d_2w_3 + d_1d_3w_2 + d_1d_2w_4 + d_1d_4w_2, \\ b &= d_1d_3w_4 + d_1d_4w_3 - k_3k_5r + d_1w_2w_3 + d_1w_2w_4 + d_1w_3w_4, \\ c &= d_1d_2d_3w_4 + d_1d_2d_4w_3 + d_1d_3d_4w_2 - d_2k_3k_5r - k_2k_4k_5r + d_1d_2w_3w_4 + d_1d_3w_2w_4, \\ d &= d_1d_4w_2w_3 - k_3k_5rw_2 + d_1w_2w_3w_4 + d_1d_2d_3d_4, \end{aligned}$$

Based on linear stability theory the local dynamics of controlled discrete Kawasaki disease model (35) about $E^0\left(\frac{r}{d_1},0,0,0\right)$, can be stated as following Lemma:

Lemma 6.1 $E^0\left(\frac{r}{d_1},0,0,0\right)$, of controlled discrete Kawasaki disease model (35) is a sink if

$$\begin{aligned} &|K_1^* + K_3^*| < 1 + K_4^* + K_2^*,\ |K_1^* - K_3^*| < 2\left(1 - K_4^*\right),\ K_2^* - 3K_4^* < 3, \\ &K_4^* + K_2^* + {K_4^*}^2 + {K_1^*}^2 + {K_4^*}^2K_2^* + K_4^*{K_3^*}^2 < 1 + 2K_4^*K_2^* + K_1^*K_3^* + K_4^*K_1^*K_3^* + {K_4^*}^3, \end{aligned} \tag{38}$$

where K_1^*, K_2^*, K_3^* and K_4^* are depicted in Eq (37).

Proof Since $J(E^0)\left(\frac{r}{d_1},0,0,0\right)$ about interior equilibrium solution $E^0\left(\frac{r}{d_1},0,0,0\right)$ of controlled discrete Kawasaki disease model (35) has characteristics polynomial which is depicted in model (36).$E^0\left(\frac{r}{d_1},0,0,0\right)$ of controlled discrete Kawasaki disease model (35) is a sink if $|K_1^* + K_3^*| < 1 + K_4^* + K_2^*$,

$|K_1^* - K_3^*| < 2\left(1 - K_4^*\right)$, and
${K_4^*}^2 + K_2^* + {K_4^*}^2 + {K_1^*}^2 + {K_4^*}^2K_2^* + K_4^*{K_3^*}^2 < 1 + 2K_4^*K_2^* + K_1^*K_3^* + K_4^*K_1^*K_3^* + {K_4^*}^3$,
$K_2^* - 3K_4^* < 3$, where K_1^*, K_2^*, K_3^* and K_4^* are depicted in Eq (37). □

Numerical scheme

Following the equation stated in (8), we get:

$$\begin{aligned} E = E_0 &+ \frac{1-\eta}{\mathscr{B}(\eta)}\rho_1(t, E(t)) + \frac{\eta}{\mathscr{B}(\eta)\Gamma(\eta)}\int_0^t (t-\upsilon)^{\eta-1}\rho_1(\upsilon, E(\upsilon))\,d\upsilon \\ &- \frac{1-\eta}{\mathscr{B}(\eta)}\rho_1(0, E(0))\left(1 + \frac{\gamma_\eta}{\Gamma(\eta+1)}t^\eta\right). \end{aligned} \tag{39}$$

With the help of[44,47], we construct a numerical approach for (39) by applying Lagrange interpolation polynomials. Substituting t_{n+1} for t yields

$$\begin{aligned} E = E_0 &+ \frac{1-\eta}{\mathscr{B}(\eta)}\rho_1(t_n, E(t_n)) + \frac{\eta}{\mathscr{B}(\eta)\Gamma(\eta)}\int_0^{t_{n+1}} (t_{n+1}-\upsilon)^{\eta-1}\rho_1(\upsilon, E(\upsilon))\,d\upsilon \\ &- \frac{1-\eta}{\mathscr{B}(\eta)}\rho_1(0, E(0))\left(1 + \frac{\gamma_\eta}{\Gamma(\eta+1)}{t_n}^\eta\right). \end{aligned} \tag{40}$$

By the Lagrange interpolation, we have

$$\begin{aligned} \rho_1(t, E(t)) &= \frac{\rho_1(t_m, E(t_m))(t - t_{m-1})}{t_m - t_{m-1}} - \frac{\rho_1(t_{m-1}, E(t_{k-1}))(t - t_m)}{t_m - t_{m-1}} \\ &= \frac{\rho_1(t_m, E(t_m))(t - t_{m-1})}{h} - \frac{\rho_1(t_{m-1}, E(t_{m-1}))(t - t_m)}{h}. \end{aligned} \tag{41}$$

By the help of (39) and (41), we have

$$
\begin{aligned}
E\left(t_{m+1}\right) = E_0 &+ \frac{1-\eta}{\mathscr{B}\left(\eta\right)}\rho_1\left(t_m, E\left(t_m\right)\right) \\
&+ \frac{\eta}{\mathscr{B}\left(\eta\right)\Gamma\left(\eta\right)}\sum_{i=1}^{n}\left[\frac{\rho_1\left(t_i, u\left(t_i\right)\right)}{h}\int_{t_m}^{t_{m+1}}\left(\upsilon - t_{i-1}\right)\left(t_{n+1}-\upsilon\right)^{\eta-1}d\upsilon\right. \\
&\left. - \frac{\rho_1\left(t_{i-1}, \varpi_i\left(t_{i-1}\right)\right)}{h}\int_{t_m}^{t_{n+1}}\left(\upsilon - t_m\right)\left(t_{n+1}-\upsilon\right)^{\eta-1}d\upsilon\right] \\
&- \frac{1-\eta}{\mathscr{B}\left(\eta\right)}\rho_1\left(0, E\left(0\right)\right)\left(1 + \frac{\gamma_\eta}{\Gamma\left(\eta+1\right)}{t_m}^{\eta}\right).
\end{aligned} \tag{42}
$$

Solving the integrals, we get

$$
\begin{aligned}
E_{m+1} = E_0 &+ \frac{1-\eta}{\mathscr{B}\left(\eta\right)}\rho_1\left(t_m, E\left(t_m\right)\right) \\
&+ \frac{\eta h^\eta}{\Gamma\left(\eta+2\right)}\sum_{j=1}^{m}\left[\rho_1\left(t_i, E\left(t_i\right)\right)\left(\left(m-j+1\right)^\eta\left(m+2-j+\eta\right)\right.\right. \\
&\left. -\left(m-i\right)^\eta\left(m+2-j+2\eta\right)\right) - \rho_1\left(t_{i-1}, E_{i-1}\right)\left(\left(m-i+1\right)^{\eta+1}\right. \\
&\left.\left. -\left(m-j+1+\eta\right)\left(m-i\right)^\eta\right)\right] - \frac{1-\eta}{\mathscr{B}\left(\eta\right)}\rho_1\left(0, E\left(0\right)\right)\left(1 + \frac{\gamma_\eta}{\Gamma\left(\eta+1\right)}\left(mh\right)^\eta\right).
\end{aligned} \tag{43}
$$

Similarly,

$$
\begin{aligned}
V_{m+1} = V_0 &+ \frac{1-\eta}{\mathscr{B}\left(\eta\right)}\rho_2\left(t_m, V\left(t_m\right)\right) \\
&+ \frac{\eta h^\eta}{\Gamma\left(\eta+2\right)}\sum_{j=1}^{m}\left[\rho_2\left(t_i, V\left(t_i\right)\right)\left(\left(m-j+1\right)^\eta\left(m+2-j+\eta\right)\right.\right. \\
&\left. -\left(m-i\right)^\eta\left(m+2-j+2\eta\right)\right) - \rho_2\left(t_{i-1}, V_{i-1}\right)\left(\left(m-i+1\right)^{\eta+1}\right. \\
&\left.\left. -\left(m-j+1+\eta\right)\left(m-i\right)^\eta\right)\right] - \frac{1-\eta}{\mathscr{B}\left(\eta\right)}\rho_1\left(0, V\left(0\right)\right)\left(1 + \frac{\gamma_\eta}{\Gamma\left(\eta+1\right)}\left(mh\right)^\eta\right),
\end{aligned} \tag{44}
$$

$$
\begin{aligned}
C_{m+1} = C_0 &+ \frac{1-\eta}{\mathscr{B}\left(\eta\right)}\rho_3\left(t_m, C\left(t_m\right)\right) \\
&+ \frac{\eta h^\eta}{\Gamma\left(\eta+2\right)}\sum_{j=1}^{m}\left[\rho_3\left(t_i, C\left(t_i\right)\right)\left(\left(m-j+1\right)^\eta\left(m+2-j+\eta\right)\right.\right. \\
&\left. -\left(m-i\right)^\eta\left(m+2-j+2\eta\right)\right) - \rho_3\left(t_{i-1}, C_{i-1}\right)\left(\left(m-i+1\right)^{\eta+1}\right. \\
&\left.\left. -\left(m-j+1+\eta\right)\left(m-i\right)^\eta\right)\right] - \frac{1-\eta}{\mathscr{B}\left(\eta\right)}\rho_3\left(0, C\left(0\right)\right)\left(1 + \frac{\gamma_\eta}{\Gamma\left(\eta+1\right)}\left(mh\right)^\eta\right),
\end{aligned} \tag{45}
$$

and

$$
\begin{aligned}
P_{m+1} = P_0 &+ \frac{1-\eta}{\mathscr{B}\left(\eta\right)}\rho_4\left(t_m, P\left(t_m\right)\right) \\
&+ \frac{\eta h^\eta}{\Gamma\left(\eta+2\right)}\sum_{j=1}^{m}\left[\rho_4\left(t_i, P\left(t_i\right)\right)\left(\left(m-j+1\right)^\eta\left(m+2-j+\eta\right)\right.\right. \\
&\left. -\left(m-i\right)^\eta\left(m+2-j+2\eta\right)\right) - \rho_4\left(t_{i-1}, P_{i-1}\right)\left(\left(m-i+1\right)^{\eta+1}\right. \\
&\left.\left. -\left(m-j+1+\eta\right)\left(m-i\right)^\eta\right)\right] - \frac{1-\eta}{\mathscr{B}\left(\eta\right)}\rho_4\left(0, C\left(0\right)\right)\left(1 + \frac{\gamma_\eta}{\Gamma\left(\eta+1\right)}\left(mh\right)^\eta\right).
\end{aligned} \tag{46}
$$

Results of proposed scheme

The temporal dynamic characteristics pertinent to the fractional-order epidemiological model for Kawasaki disease (8) are examined through the numerical simulations delineated in this section. It is crucial to show that the presented work is feasible and to use large-scale numerical simulation to verify the analytical work's correctness. For a range of fractional values dependent on the steady-state point, the model numerical results are computed using Atangana-Baleanu in the Caputo sense in conjunction with Mittag-

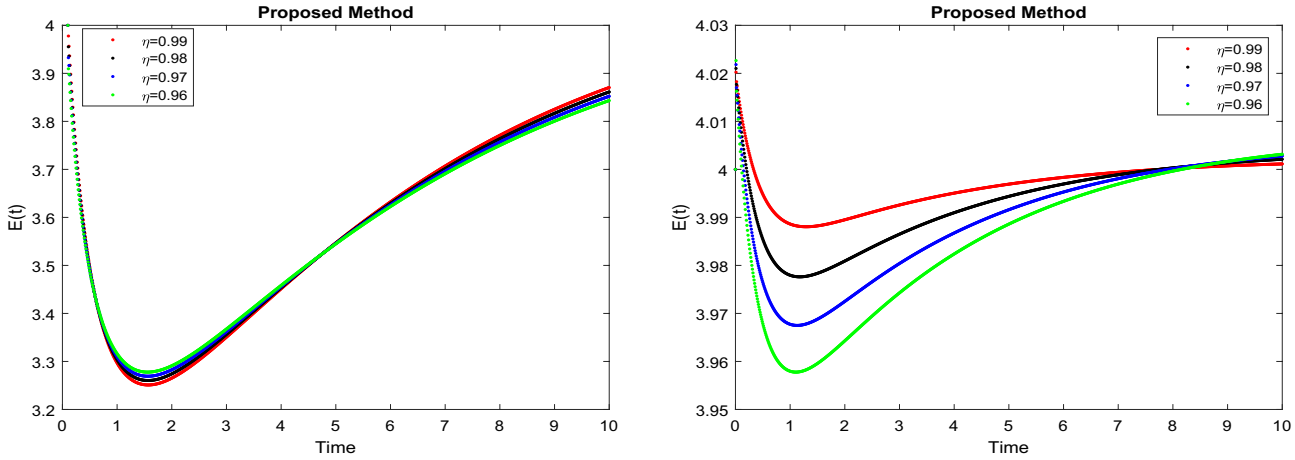

(a) ABC (b) MABC

Fig. 4. Simulation of $E(t)$ when $R_0 < 1$ with parametric value of η.

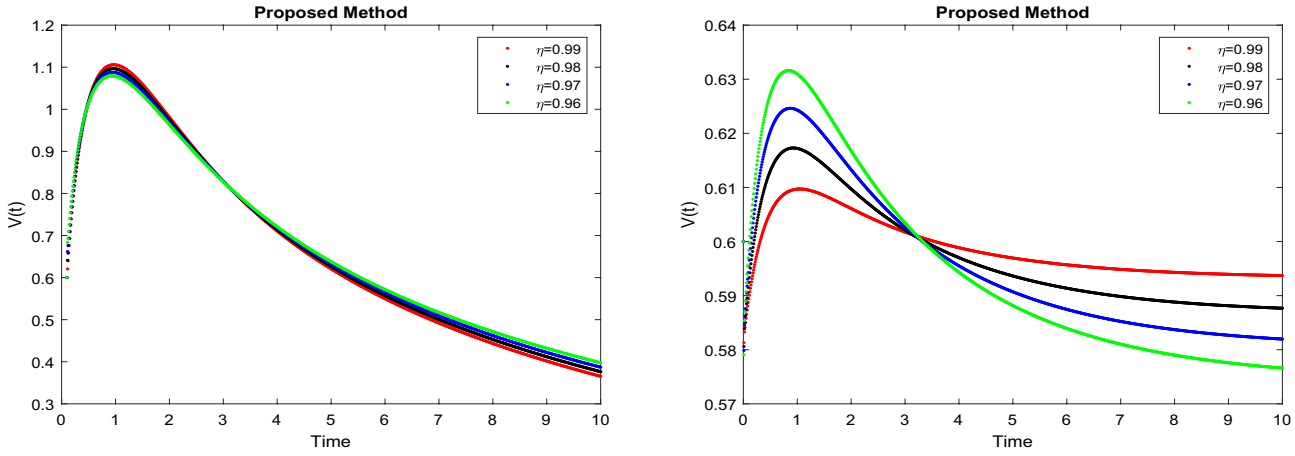

(a) ABC (b) MABC

Fig. 5. Simulation of $V(t)$ when $R_0 < 1$ with parametric value of η.

Leffler law. These simulations show how a change in value affects the model behavior. Furthermore, the results for fractional values demonstrate higher efficiency as compared to the usual derivative. It enables a more accurate estimation of the best amount for disease control. The actual parameters of the data are $r = 2, d_1 = 0.5, d_2 = 1, d_3 = 1, d_4 = 1, k_1 = 1, k_2 = 0.1, k_3 = 1, k_4 = 0.5, k_5 = 0.16, k_6 = 0.45$ [23]. The nature of time in a days. The Kawasaki disease model dynamics for various values of $t \in [0, 10]$ are depicted in Figures 4a, 5a, 6a, and 7a, which use the Atangana-Baleanu type non-singular fractional derivative. Figures 4b, 5b, 6b, and 7b demonstrate the dynamics of the Kawasaki disease model for different values of $t \in (0, 1)$ using the non-singular fractional derivative of the Modified Atangana-Baleanu type. Figure 4 illustrates the $E(t)$ dynamics for different fractional orders, showing that lower fractional orders correspond to increased endothelial cell populations over time. This could relate to heightened cellular proliferation from vascular endothelial growth factors, potentially leading to vascular issues seen in Kawasaki disease. This indicates the possibility of targeting endothelial proliferation to reduce vascular damage. The $V(t)$ dynamics shown in Figure 5 indicate that as fractional orders η increase, the population of classes decreases. A decline in $V(t)$ levels at higher fractional orders may dampen the growth and repair of vascular tissues, potentially weakening endothelial function and increasing vulnerability to inflammation. This suggests that $V(t)$ modulation could be a therapeutic avenue, as lower $V(t)$ may correlate with disease remission phases. The dynamics of $C(t)$ are shown in Figure 6 for various fractional orders η. Higher fractional orders lead to a continuous decrease in the population of classes and chemokine levels, indicating a reduced immune response in severe disease stages. This suggests that managing chemokine levels may influence immune cell recruitment, potentially helping to control inflammation and disease severity. Figure 7 shows that as the fractional order η decreases, the class population $P(t)$ steadily rises. Inflammatory factors increase, particularly at lower fractional orders, indicating

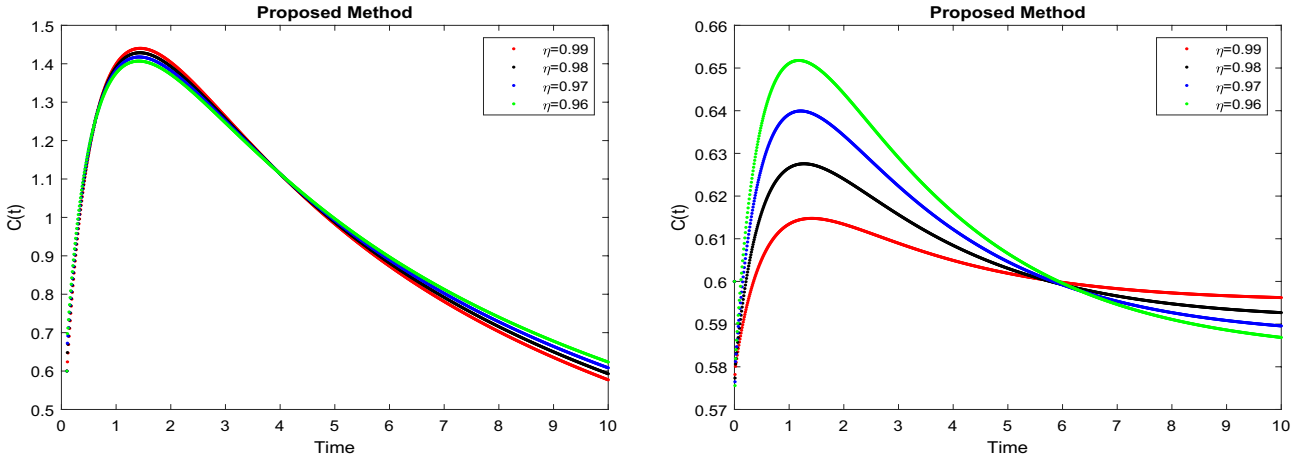

Fig. 6. Simulation of $C(t)$ when $R_0 < 1$ with parametric value of η.

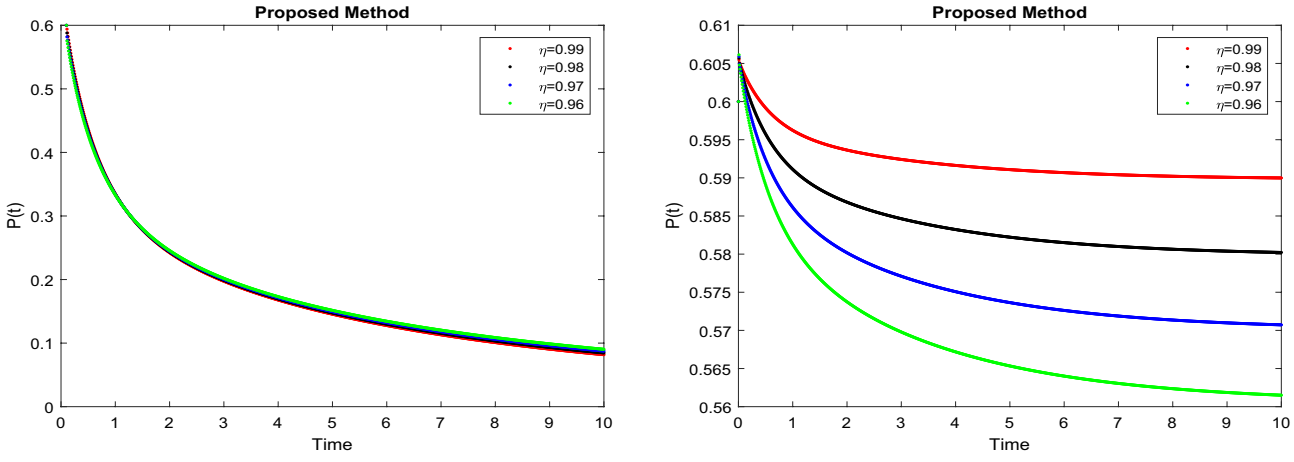

Fig. 7. Simulation of $P(t)$ when $R_0 < 1$ with parametric value of η.

ongoing inflammation typical of Kawasaki disease. This persistent inflammation may lead to further vascular damage and greater disease severity, highlighting the need for early anti-inflammatory interventions. The trends in Figures 4, 5, 6, and 7 indicate that lower fractional orders result in heightened and sustained levels of inflammatory factors (P) and endothelial cells (E), suggesting more aggressive disease progression. Higher fractional orders reduce these levels, implying a dampening effect on inflammation. This implies that manipulating fractional orders could help modulate disease severity, offering potential control points for Kawasaki disease interventions. The crossover behavior in Figures 4, 5, 6, and 7 suggests a shift in the influence of fractional orders on the dynamics of each variable, reflecting transitions between different phases of Kawasaki disease. This behavior aligns with real-life disease progression, where initial inflammatory responses peak and later decline due to regulatory mechanisms. Such transitions validate the model's ability to capture complex disease stages, confirming its realism and robustness for simulating Kawasaki disease dynamics. To demonstrate that fractional derivatives better capture Kawasaki disease dynamics, simulate both fractional and integer-order models. The fractional model shows a gradual decline in inflammation levels, reflecting the persistent inflammatory response in Kawasaki disease, while the integer model indicates a quicker decline. Compare to previous study[23] simulations reveal that the fractional-order model exhibits more nuanced dynamics, such as delayed responses and complex transient behaviors, aligning better with real-world biological data. By comparing graphs, it is evident that the MABC model aligns more closely with realistic biological processes, making it a better choice for simulating complex disease dynamics like Kawasaki disease. For public health policy, these findings provide evidence that fractional-order models could improve predictions of Kawasaki disease outcomes and help design

targeted therapies, especially during early stages. This model could guide resource allocation in clinical settings by highlighting which biological processes to monitor closely in Kawasaki disease patients.

Conclusion

We examine the interactions between different parameters in the Kawasaki disease model (8) in this article. We analyze the dynamic behavior of the system for constant controls by using the fractional operator Kawasaki disease model. We took into consideration the recently developed modified ABC operator in our proposed problem. The modified Atangana-Baleanu-Caputo operator offers advantages over the standard Atangana-Baleanu-Caputo operator in terms of well-posedness and initialization. The MABC operator addresses initialization issues present in the ABC operator, leading to more robust and reliable model simulations. This improved initialization contributes to a more accurate representation of Kawasaki disease dynamics. Consequently, the MABC operator provides a more effective framework for analyzing the model's stability and control. We assert that this operator has afforded researchers a novel pathway for investigation within their scholarly endeavors. The application of Leray-Schauder method was employed to ascertain the existence of solutions. The examination of the global stability of the fractional order model is conducted through the utilization of the Lyapunov function. This new numerical method was developed and used for a Kawasaki disease mathematical model using Lagrange's interpolation polynomial. We pointed out that the results are more realistic and that the approach can be used to examine dynamical systems in more detail. The effect of fractional order on the analysis of vaccination and community effects is demonstrated using a numerical simulation. According to this study, the ABC model yields less insightful results on compartmental population dynamics than the MABC fractional-order model. Therefore, it may be said that MABC is particularly useful for simulating real-world issues. Readers might review the imagined problem by using additional fixed-point approaches to see if there are multiple or unique solutions. Additionally, they might develop new numerical systems using other techniques. Future work could extend this model by incorporating additional biological complexities, such as immune system interactions, environmental factors, or genetic predispositions, to enhance its applicability to Kawasaki disease. The framework could also be adapted to model other diseases with similar dynamics, like rheumatoid arthritis or systemic vasculitis, by adjusting parameters and fractional orders. Exploring advanced numerical methods, such as adaptive or hybrid techniques, could improve computational efficiency and accuracy for complex systems. Collaborative efforts with clinical researchers could further validate and refine the model for real-world applications.

Data availability

The datasets analyzed during the current study are available from the corresponding author upon reasonable request.

Received: 14 September 2024; Accepted: 1 July 2025
Published online: 17 July 2025

References

1. Kawasaki, T., Kosaki, F., Okawa, S., Shigematsu, I. & Yanagawa, H. A new infantile acute febrile mucocutaneous lymph node syndrome (MLNS) prevailing in Japan. *Pediatrics* **54**(3), 271–276 (1974).
2. Newburger, J. W., Takahashi, M. & Burns, J. C. Kawasaki disease. *J. Am. Coll. Cardiol.* **67**(14), 1738–1749 (2016).
3. Newburger, J. W. et al. Diagnosis, treatment, and long-term management of Kawasaki disease: A statement for health professionals from the Committee on Rheumatic Fever, Endocarditis and Kawasaki Disease, Council on Cardiovascular Disease in the Young. *Am. Heart Assoc. Circ.* **110**(17), 2747–2771 (2004).
4. Singh, S., Vignesh, P. & Burgner, D. The epidemiology of Kawasaki disease: A global update. *Arch. Dis. Childhood* **100**(11), 1084–1088 (2015).
5. Gordon, J. B., Kahn, A. M. & Burns, J. C. When children with Kawasaki disease grow up: Myocardial and vascular complications in adulthood. *J. Am. Coll. Cardiol.* **54**(21), 1911–1920 (2009).
6. Gordon, J. B. et al. The spectrum of cardiovascular lesions requiring intervention in adults after Kawasaki disease. *JACC Cardiovasc. Interv.* **9**(7), 687–696 (2016).
7. Rosenkranz, M. E. et al. TLR2 and MyD88 Contribute to Lactobacillus casei extract-induced focal coronary arteritis in a mouse model of kawasaki disease. *Circulation* **112**(19), 2966–2973 (2005).
8. Schulte, D. J. et al. Involvement of innate and adaptive immunity in a murine model of coronary arteritis mimicking Kawasaki disease. *J. Immunol.* **183**(8), 5311–5318 (2009).
9. Rowley, A. H., Baker, S. C., Orenstein, J. M. & Shulman, S. T. Searching for the cause of Kawasaki disease-cytoplasmic inclusion bodies provide new insight. *Nat. Rev. Microbiol.* **6**(5), 394–401 (2008).
10. Rowley, A. H. et al. Ultrastructural, immunofluorescence, and RNA evidence support the hypothesis of a "new" virus associated with Kawasaki disease. *J. Infect. Dis.* **203**(7), 1021–1030 (2011).
11. Newburger, J. W. et al. Diagnosis, treatment, and long-term management of Kawasaki disease: A statement for health professionals from the Committee on Rheumatic Fever, Endocarditis and Kawasaki Disease, Council on Cardiovascular Disease in the Young. *Am. Heart Assoc. Circ.* **110**(17), 2747–2771 (2004).
12. Tremoulet, A. H. et al. Resistance to intravenous immunoglobulin in children with Kawasaki disease. *J. Pediatr.* **153**(1), 117–121 (2008).
13. Kato, H. et al. Long-term consequences of Kawasaki disease: A 10-to 21-year follow-up study of 594 patients. *Circulation* **94**(6), 1379–1385 (1996).
14. Friedman, K. G. et al. Coronary artery aneurysms in Kawasaki disease: Risk factors for progressive disease and adverse cardiac events in the US population. *J. Am. Heart Assoc.* **5**(9), e003289 (2016).
15. Burns, J. C. & Franco, A. The immunomodulatory effects of intravenous immunoglobulin therapy in Kawasaki disease. *Expert Rev. Clin. Immunol.* **11**(7), 819–825 (2015).
16. Skochko, S. M. et al. Kawasaki disease outcomes and response to therapy in a multiethnic community: A 10-year experience. *J. Pediatr.* **203**, 408–415 (2018).
17. Makino, N. et al. Nationwide epidemiologic survey of Kawasaki disease in Japan, 2015–2016. *Pediatr. Int.* **61**(4), 397–403 (2019).
18. Takahashi, K., Oharaseki, T., Yokouchi, Y., Hiruta, N. & Naoe, S. Kawasaki disease as a systemic vasculitis in childhood. *Ann. Vasc. Dis.* **3**(3), 173–181 (2010).

19. Takahashi, K., Oharaseki, T. & Yokouchi, Y. Histopathological aspects of cardiovascular lesions in Kawasaki disease. *Int. J. Rheum. Dis.* **21**(1), 31–35 (2018).
20. Brown, T. J. et al. CD8 T lymphocytes and macrophages infiltrate coronary artery aneurysms in acute Kawasaki disease. *J. Infect. Dis.* **184**(7), 940–943 (2001).
21. Rowley, A. H., Eckerley, C. A., Shulman, J. H. M. & Baker, S. C. IgA plasma cells in vascular tissue of patients with Kawasaki syndrome. *J. Immunol.* **159**(12), 5946–5955 (1997).
22. Rowley, Anne H. et al. IgA plasma cell infiltration of proximal respiratory tract, pancreas, kidney, and coronary artery in acute Kawasaki disease. *J. Infect. Dis.* **182**(4), 1183–1191 (2000).
23. Leung, D. Y. et al. Two monokines, interleukin 1 and tumor necrosis factor, render cultured vascular endothelial cells susceptible to lysis by antibodies circulating during Kawasaki syndrome. *J. Exp. Med.* **164**(6), 1958–1972 (1986).
24. Leung, D. M. et al. Endothelial cell activation and high interleukin-1 secretion in the pathogenesis of acute Kawasaki disease. *The Lancet* **334**(8675), 1298–1302 (1989).
25. Caputo, M. Linear models of dissipation whose Q is almost frequency independent-II. *Geophys. J. Int.* **13**(5), 529–539 (1967).
26. Caputo, M. & Fabrizio, M. A new definition of fractional derivative without singular kernel. *Prog. Fract. Differ. Appl.* **1**(2), 73–85 (2015).
27. Atangana, A. & Baleanu, D. New fractional derivatives with nonlocal and non-singular kernel: Theory and application to heat transfer model. *Therm. Sci.* **20**(2), 763–9 (2016).
28. Al-Refai, M. & Baleanu, D. On an extension of the operator with Mittag-Leffler kernel. *Fractals* **30**(05), 2240129 (2022).
29. Farman, M., Jamil, K., Xu, C., Nisar, K. S. & Amjad, A. Fractional order forestry resource conservation model featuring chaos control and simulations for toxin activity and human-caused fire through modified ABC operator. *Math. Comput. Simul.* **227**, 282–302 (2024).
30. Jamil, S., Naik, P. A., Farman, M., Saleem, M. U. & Ganie, A. H. Stability and complex dynamical analysis of COVID-19 epidemic model with non-singular kernel of Mittag-Leffler law. *J. Appl. Math. Comput.* **70**, 3441 (2024).
31. Nisar, K. S., Farman, M., Abdel-Aty, M. & Ravichandran, C. A review of fractional order epidemic models for life sciences problems: Past, present and future. *Alex. Eng. J.* **95**, 283–305 (2024).
32. Khan, A. et al. Fractional dynamics and stability analysis of COVID-19 pandemic model under the harmonic mean type incidence rate. *Comput. Methods Biomech. Biomed. Eng.* **25**(6), 619–640 (2022).
33. Khan, A. et al. Modeling and sensitivity analysis of HBV epidemic model with convex incidence rate. *Results Phys.* **22**, 103836 (2021).
34. Zarin, R., Khan, A. & Akg, L. A. Fractional modeling of COVID-19 pandemic model with real data from Pakistan under the ABC operator. *AIMS Math.* **7**(9), 15939–15964 (2022).
35. Yu, D., Liao, X. & Wang, Y. Modeling and analysis of Caputo Fabrizio definition-based fractional-order boost converter with inductive loads. *Fractal Fract.* **8**(2), 81 (2024).
36. Xu, K. et al. Fractional-order Zener model with temperature-order equivalence for viscoelastic dampers. *Fractal Fract.* **7**(10), 714 (2023).
37. Ali, Z., Rabiei, F., Rashidi, M. M. & Khodadadi, T. A fractional-order mathematical model for COVID-19 outbreak with the effect of symptomatic and asymptomatic transmissions. *Eur. Phys. J.Plus* **137**(3), 395 (2022).
38. Farman, M., Shehzad, A., Nisar, K. S., Hincal, E. & Akgul, A. A mathematical fractal-fractional model to control tuberculosis prevalence with sensitivity, stability, and simulation under feasible circumstances. *Comput. Biol. Med.* **178**, 108756 (2024).
39. Xu, C. et al. New results on bifurcation for fractional-order octonion-valued neural networks involving delays. *Netw. Comput. Neural Syst.* https://doi.org/10.1080/0954898X.2024.2332662 (2024).
40. Xu, C. et al. Bifurcation investigation and control scheme of fractional neural networks owning multiple delays. *Comput. Appl. Math.* **43**(4), 1–33 (2024).
41. Khan, H., Alzabut, J., Alfwzan, W. F. & Gulzar, H. Nonlinear dynamics of a piecewise modified ABC fractional-order leukemia model with symmetric numerical simulations. *Symmetry* **15**(7), 1338 (2023).
42. Khan, H., Alzabut, J., G-Aguilar, J. F. & Alkhazan, A. Essential criteria for existence of solution of a modified-ABC fractional order smoking model. *Ain Shams Eng. J.* **15**(5), 102646 (2024).
43. Khan, H., Alzabut, J., Almutairi, D. K. & Alqurashi, W. K. The use of artificial intelligence in data analysis with error recognitions in liver transplantation in HIV-AIDS patients using modified ABC fractional order operators. *Fractal Fract.* **9**(1), 16 (2024).
44. Khan, H., Alzabut, J., Baleanu, D., Alobaidi, G. & Rehman, M. U. Existence of solutions and a numerical scheme for a generalized hybrid class of n-coupled modified ABC-fractional differential equations with an application. (2023).
45. Paul, S., Mahata, A., Mukherjee, S. & Roy, B. Dynamics of SIQR epidemic model with fractional order derivative. *Partial Differ. Equ. Appl. Math.* **5**, 100216 (2022).
46. Dano, L. B., Koya, P. R. & Keno, T. D. Fractional optimal control strategies for hepatitis B virus infection with cost-effectiveness analysis. *Sci. Rep.* **13**(1), 19514 (2023).
47. Al-Refai, M. & Baleanu, D. On an extension of the operator with Mittag-Leffler kernel. *Fractals* **30**(05), 2240129 (2022).

Acknowledgements

This study is supported via funding from Prince Sattam bin Abdulaziz University project number (PSAU/2025/R/1446).

Competing interests

The authors declare that they have no conflict of interest.

Additional information

Correspondence and requests for materials should be addressed to M.F.

Reprints and permissions information is available at www.nature.com/reprints.

Publisher's note Springer Nature remains neutral with regard to jurisdictional claims in published maps and institutional affiliations.